

Supporting Information

Blocquet et al. 10.1073/pnas.1314968110

SI Text

Additional Details About the Experimental Facility

The oxidation of *n*-butane was performed using a spherical fused silica jet-stirred reactor (JSR). This is an isothermal and isobaric continuous flow reactor working under steady state, which is well adapted to kinetic studies. It was designed to obtain homogeneous concentrations and temperatures of the gas phase inside the reactor for residence times between 0.5 and 10 s. Radicals exiting the reactor were analyzed by Fluorescence Assay by Gas Expansion (FAGE).

The JSR. This type of reactor was already used for numerous gas-phase kinetic studies (e.g., refs. 1–3). Fig. S1 shows the reactor before the insertion of the sampling cone-like nozzle. It is a spherical reactor in which diluted reactants enter through an injection cross located in its center. The diameter of the reactor is about 55 mm and its volume is about 88 cm³. It can be considered as well stirred for a mean residence time (τ) between 0.5 and 10 s (in the latter case, the Reynolds number is 1,070 and the recirculation ratio 127) (4). The stirring of the whole reactor volume is achieved by the mean of four turbulent gas jets injected into the reactor in different directions and produced by the four nozzles of the injection cross in the center of the reactor. Inside diameter of the nozzles is about 0.3 mm.

The quartz reactor is preceded by a quartz annular preheating zone in which the temperature of the gas is increased up to the reactor temperature before being injected into the reactor. The annular preheater is made of two concentric tubes, the inter-annular distance of which is about 0.5 mm. The residence time of the gas mixture inside the annular preheater is very short compared with its residence time inside the reactor (about a few percent). Both spherical reactor and annular preheating zone are heated by the mean of “Thermocoax” heating resistances rolled up around their wall. Reaction temperature measurement is made by means of a thermocouple K (Thermocoax), which is located inside the intraannular space of the preheating zone and the extremity being placed at the level of the injection cross. One other thermocouple is placed between the heating resistances and the reactor wall for temperature regulation (Fig. S1). The dilution was large enough so that a maximum temperature increase of 5 K with respect to the set temperature is obtained due to exothermicity of the reaction when starting the reactive gases feeding. The temperatures are controlled by a multi-channel regulator (HORST). The gases were provided by Messer (purity of 99.95%). Gas flows were controlled by Bronkhorst mass flow controllers.

FAGE Analysis. The University of Lille FAGE (UL-FAGE) instrument has been detailed previously and shall be described only briefly here. It is designed to determine the absolute concentration of $\bullet\text{OH}$ and $\bullet\text{HO}_2$ in the atmosphere. Its measurement principle is based on laser-induced fluorescence (LIF) of $\bullet\text{OH}$ collected around 308 nm [A-X (0-0)] at low pressure (0.5 torr) after an excitation by a high repetition rate dye laser (Sirah Precision Scan) at 308.244 nm [Q₁(3)]. The fluorescence signal can be temporally separated from the excitation thanks to the low pressure, reducing the quenching and increasing the fluorescence lifetime. To achieve these conditions, the ambient air (in this experiment, the outlet of the JSR) is pumped continuously through a 400- μm aperture into the cells at a flow rate of around 1.2 L/min (see further down). This nozzle is connected to a White cell to

directly detect $\bullet\text{OH}$, while NO can be added a few centimeters downstream of the inlet orifice to convert $\bullet\text{HO}_2$ into $\bullet\text{OH}$.

The LIF signal from the excited $\bullet\text{OH}$ is detected perpendicular to the excitation beam and quantified by photon counting using a gated Channel Photon Multiplier module (Perkin-Elmer).

The measurement cycle consists in 20-s “ON” resonance, i.e., on the $\bullet\text{OH}$ peak to measure the fluorescence, followed by 20-s “OFF” resonance to measure the background, and 20 s to go back to the ON resonance conditions. This method allows to account only for fluorescence photons, which stem from $\bullet\text{OH}$ radicals, i.e., any fluorescence photons due to a broadband fluorescence of other species in the reaction mixture, i.e., polycyclic aromatic hydrocarbons, would be subtracted by this method. The wavelength of the laser is kept precisely on the $\bullet\text{OH}$ peak using a reference cell where a stable concentration of $\bullet\text{OH}$ radicals is produced by thermolysis of water: a small fraction of the laser beam is deviated into this reference cell and the fluorescence intensity measured in the reference cell served as control for the long-term stability of the $\bullet\text{OH}$ fluorescence signal.

To access the absolute concentrations, calibrations are made using a calibration cell in which air with a known water vapor concentration is photolysed at 184.9 nm by a mercury lamp, producing an equal and known concentration of $\bullet\text{OH}$ and $\bullet\text{HO}_2$. The lamp flux is indirectly measured by actinometry on ozone, produced simultaneously by oxygen photolysis at the same wavelength.

The detection limit of the instrument is on the order of 3.7×10^5 molecule·cm⁻³ on $\bullet\text{OH}$, for a time resolution of 1 min. The detection limit for $\bullet\text{HO}_2$ radicals is somewhat lower, because the conversion of $\bullet\text{HO}_2$ into $\bullet\text{OH}$ is not complete: therefore, the detection limit depends on the added NO concentration (see further down). However, radical concentrations in combustion systems are many orders of magnitude higher than in the atmosphere, and this is especially true for $\bullet\text{HO}_2$ radicals. Therefore, the sensitivity of the instrument had to be drastically lowered to avoid saturation of the signal. Two methods for attenuating the sensitivity of the instrument have been used:

- i) the energy of the fluorescence excitation laser has been decreased by a factor of 2 compared with the “atmospheric” configuration when measuring $\bullet\text{OH}$ radical profiles and by an additional factor of 30 for all $\bullet\text{HO}_2$ measurements using neutral density filters, and
- ii) very low NO concentration have been used for converting $\bullet\text{HO}_2$ into $\bullet\text{OH}$, leading to a decrease in sensitivity for the $\bullet\text{HO}_2$ detection.

The reaction time for NO with the $\bullet\text{HO}_2$ radicals is relatively short (a few milliseconds); therefore, the conversion rate increases with increasing NO concentration. This increase levels off at high NO concentrations when all $\bullet\text{HO}_2$ radicals are converted into $\bullet\text{OH}$. In Fig. S2 is shown the evolution of the fluorescence signal obtained at a constant temperature (643 K) as a function of NO concentration. The use of such low NO concentration has also the advantage that a possible interference due to RO₂ radicals, present in the reaction mixtures, is decreased to a minimum. As has been shown by Fuchs et al. (5), RO₂ radicals can, depending on their structure, lead to an interference within the FAGE, if high NO concentrations are used, that allow the two-step conversion of RO₂ + NO → RO + NO₂, followed by RO + O₂ → R'_(-H)O + $\bullet\text{HO}_2$, followed by $\bullet\text{HO}_2$ + NO → $\bullet\text{OH}$ + NO₂.

For $\bullet\text{OH}$ radicals, a calibration carried out under the conditions of the JSR experiments yielded a sensitivity of $f_{\bullet\text{OH}} = 3 \times 10^7$ $\bullet\text{OH}$ cm⁻³·cts⁻¹ for the FAGE system. Furthermore, the dilution of the

JSR exhaust by a factor of 2.6–5.2 with ambient air (see further down) has to be taken into account to obtain an estimation of the absolute concentration. As it has been explained before, a direct calibration with an atmospheric calibration source is not reliable, especially for $\bullet\text{HO}_2$ radicals. Therefore, rather than determining directly a calibration factor $f_{\bullet\text{HO}_2}$, we have derived the calibration factor ($f_{\bullet\text{HO}_2}$) from the above ($f_{\bullet\text{OH}}$): with the low NO concentration used to attenuate the signal, only around 20% of all $\bullet\text{HO}_2$ radicals are converted to $\bullet\text{OH}$ radicals (Fig. S2). Together with the attenuated laser excitation energy (factor 30 for $\bullet\text{HO}_2$ measurements compared with $\bullet\text{OH}$ measurements), the following relationship is obtained:

$$f_{\bullet\text{HO}_2} = f_{\bullet\text{OH}} \times \frac{30}{0.2} = f_{\bullet\text{OH}} \times 150. \quad [\text{S1}]$$

To validate this relationship, we have measured the $\bullet\text{HO}_2$ concentration by both methods: direct by using the “ $\bullet\text{OH}$ laser energy” and by attenuating the energy. This has been repeated at three temperatures where radical concentrations were rather low to not saturate the signal under the “ $\bullet\text{OH}$ laser energy” conditions. For all three temperatures, we have found a difference of less than 30% between the $\bullet\text{HO}_2$ concentration directly measured and the $\bullet\text{HO}_2$ concentration such as obtained from the above estimation.

The gas flow into the JSR is regulated by calibrated flow meters and determines the residence time of the gas mixture. In this work, a residence time of 6 s has been chosen, corresponding to flows between 460–230 $\text{cm}^3\cdot\text{min}^{-1}$ standard temperature and pressure in the temperature range 500–1,000 K, respectively, i.e., the gas flow into the JSR at 500 K is twice as high than at 1,000 K. This leads to different corrections to convert the relative LIF signals into a radical mole fraction:

- i) the gas intake of the FAGE is much higher than the gas outlet of the JSR, i.e., the gas from the JSR is diluted by ambient air during the expansion into the FAGE. Therefore, if the gas flow out of the JSR changes with changing reactor temperature, this dilution factor changes as well.
- ii) The expansion into the FAGE system is supersonic, and therefore the gas intake is not only determined by the size of the orifice and the pressure difference between ambient and FAGE cell (maintained at around 0.5 torr through constant, high pumping capacity), but also by the flow velocity of the gas. In addition, as the flow velocity of a supersonic expansion depends on heat capacity, the average flow velocity for helium is much higher than for N_2 . Gas from the JSR consists of mostly helium, and considering that the entire JSR gas flow is sampled into the FAGE, the fraction of helium in the gas mixture expanded into the FAGE increases with decreasing JSR temperature. With the pumping capacity being constant for all experiments, this results in an increased pressure within the FAGE cell with decreasing JSR temperature.

To correct for these sampling issues, the total flow into the FAGE cell should be known at each temperature. It is, however, not straightforward to neither directly measure it nor to calculate it from fluid dynamics (the temperature of the gas mixture before expansion is not well known). Therefore, we have estimated the FAGE intake for helium and for air as follows: the limiting FAGE pressure for pure He has been determined by flooding the protection cylinder with 11 $\text{L}\cdot\text{min}^{-1}$ of He and has been 0.55 torr, indicated by the dashed line in Fig. S3. The limiting pressure for pure, ambient air has been found as 0.33 torr. By adding increasing flows of He through the JSR, the expanded gas contains more and more He and the pressure within the FAGE increases. This increase is nearly linear and reaches the maximal pressure at 2 $\text{L}\cdot\text{min}^{-1}$ (Fig. S3). We therefore estimate that the intake of the FAGE consists of 2 $\text{L}\cdot\text{min}^{-1}$ pure He. From the ratio of the

FAGE pressures in pure He and air, we estimate from proportionality a total flow of air of 1.2 $\text{L}\cdot\text{min}^{-1}$. Hence, under the assumption that the entire outlet of the JSR (460–230 $\text{cm}^3\cdot\text{min}^{-1}$) is sampled into the FAGE, the difference of 0.74–0.97 $\text{L}\cdot\text{min}^{-1}$ is compensated for by intake of ambient air. Therefore, the gas from the JSR is diluted by a factor of 2.6 (500 K) to 5.2 (1,000 K). The small pressure drop in the FAGE with increasing temperature in the JSR (around 10% between 500 and 1,000 K) is taken into account by simple proportionality, i.e., a LIF signal at 1,000 K and 0.36 torr translates into a 10% lower $\bullet\text{OH}$ concentration than the same LIF signal at 500 K and 0.33 torr (the small change in quenching is neglected). This correction, however, is very small compared with the uncertainty linked to the dilution factor as well as the possible losses of radicals between JSR exhaust and FAGE expansion.

Once the LIF signals have been converted into absolute radical concentrations by applying the calibration factors $f_{\bullet\text{OH}}$ and $f_{\bullet\text{HO}_2}$ as well as the correction for dilution and FAGE pressure, the radical concentrations are converted into mole fractions by taking into account the different densities within the JSR at different temperatures.

Description of the Model Used for Simulations

The simulations were performed using the software PSR of CHEMKIN (6). The mechanism of the low-temperature oxidation of *n*-butane (available on request) has been automatically generated using EXGAS software. This software has already been used for generating mechanisms in the case of a wide range of alkanes (7, 8) and alkenes (9). The reaction mechanisms generated by EXGAS are made of three parts:

- A comprehensive primary mechanism, where the only molecular reactants considered are the initial organic compounds and oxygen. According to the reaction scheme of the oxidation of alkanes described in the main text of this paper, the reactant and the primary radicals are systematically submitted to different types of following elementary steps:
 - Unimolecular initiations involving the breaking of a C—C bond.
 - Bimolecular initiations with oxygen to produce alkyl and $\bullet\text{HO}_2$ radicals.
 - Oxidations of alkyl radicals with O_2 to form alkenes and $\bullet\text{HO}_2$ radicals.
 - Additions of alkyl (R \bullet) and hydroperoxyalkyl ($\bullet\text{QOOH}$) radicals to an oxygen molecule.
 - Isomerizations of alkyl and peroxy radicals (ROO \bullet and $\bullet\text{OOQOOH}$) involving a cyclic transition state for $\bullet\text{OOQOOH}$ radicals ($\bullet\text{QOOH}$ and $\bullet\text{OOQOOH}$ are reactive intermediates in the succession of elementary steps, represented as dotted arrows in Fig. 1).
 - Decompositions of radicals by β -scission involving the breaking of C—C or C—O bonds for all types of radicals (for low-temperature modeling, the breaking of C—H bonds is neglected).
 - Decompositions of hydroperoxyalkyl radicals to form cyclic ethers and $\bullet\text{OH}$ radicals.
 - Metatheses involving H abstractions by radicals from the initial reactants.
 - Recombinations of radicals.
 - Disproportionations of peroxyalkyl radicals with $\bullet\text{HO}_2$ to produce alkyhydroperoxides and O_2 (disproportionations between two peroxyalkyl radicals or between peroxyalkyl and alkyl radicals are not taken into account).
- A C₀—C₂ reaction base, including all of the reactions involving radicals or molecules containing less than three carbon atoms. The fact that no generic rule can be derived for the generation of the reactions involving all compounds containing less than three carbon atoms makes this reaction base necessary.

- A lumped secondary mechanism, containing the reactions consuming the C₃–C₄ molecular stable products of the primary mechanism. For reducing the number of reactants in the secondary mechanism, the molecules formed in the primary mechanism, with the same molecular formula and the same functional groups, are lumped into one unique species, without distinguishing between the different isomers. The writing of secondary reactions is made to promote the formation of C₂₊ alkyl radicals, the reactions of which are already included in the primary mechanism (8).

Thermochemical data for molecules or radicals were automatically calculated and stored as 14 polynomial coefficients, according

1. Bounaceur R, Da Costa I, Fournet R, Billaud F, Battin-Leclerc F (2005) Experimental and modeling study of the oxidation of toluene. *Int J Chem Kinet* 37(1):25–49.
2. Biet J, Hakka MH, Warth V, Glaude PA, Battin-Leclerc F (2008) Experimental and modeling study of the low-temperature oxidation of large alkanes. *Energy Fuels* 22(4):2258–2269.
3. Hakka MH, Glaude PA, Herbinet O, Battin-Leclerc F (2009) Experimental study of the oxidation of large surrogates for diesel and biodiesel fuels. *Combust Flame* 156(11): 2129–2144.
4. Matras D, Villerma J (1973) Continuous reactor perfectly agitated by gas jets for kinetic study on rapid chemical reactions. *Chem Eng Sci* 28(1):129–137.
5. Fuchs H, et al. (2011) Detection of HO₂ by laser-induced fluorescence: Calibration and interferences from RO₂ radicals. *AMT* 4(6):1209–1225.
6. Pousse E, Tian ZY, Glaude PA, Fournet R, Battin-Leclerc F (2010) A lean methane premixed laminar flame doped with components of diesel fuel. Part III: Indane and comparison between n-butylbenzene, n-propylcyclohexane and indane. *Combust Flame* 157(7):1236–1260.
7. Buda F, et al. (2005) Progress toward a unified detailed kinetic model for the autoignition of alkanes from C-4 to C-10 between 600 and 1200 K. *Combust Flame* 142(1-2):170–186.
8. Warth V, et al. (1998) Computer-aided derivation of gas-phase oxidation mechanisms: Application to the modeling of the oxidation of n-butane. *Combust Flame* 114(1-2): 81–102.
9. Touchard S, et al. (2005) Modeling of the oxidation of large alkenes at low temperature. *Proc Combust Inst* 30:1073–1081.
10. Muller C, Michel V, Scacchi G, Come GM (1995) Thergas—a computer-program for the evaluation of thermochemical data of molecules and free-radicals in the gas-phase. *J Chim Phys* 92(5):1154–1178.
11. Benson SW (1976) *Thermochemical Kinetics* (Wiley, New York), 2nd Ed.

to the CHEMKIN II formalism (6). These data were automatically calculated using software THERGAS (10), based on the group and bond additivity methods proposed by Benson (11).

The kinetic data of isomerizations, recombinations, and the unimolecular decompositions are automatically calculated using KINGAS (8) and are based on the thermochemical kinetics methods (11) using the transition state theory or the modified collision theory. The kinetic data, for which the calculation is not possible by KINGAS (8), are estimated from correlations based on quantitative structure–reactivity relationships and obtained from a literature review (7).

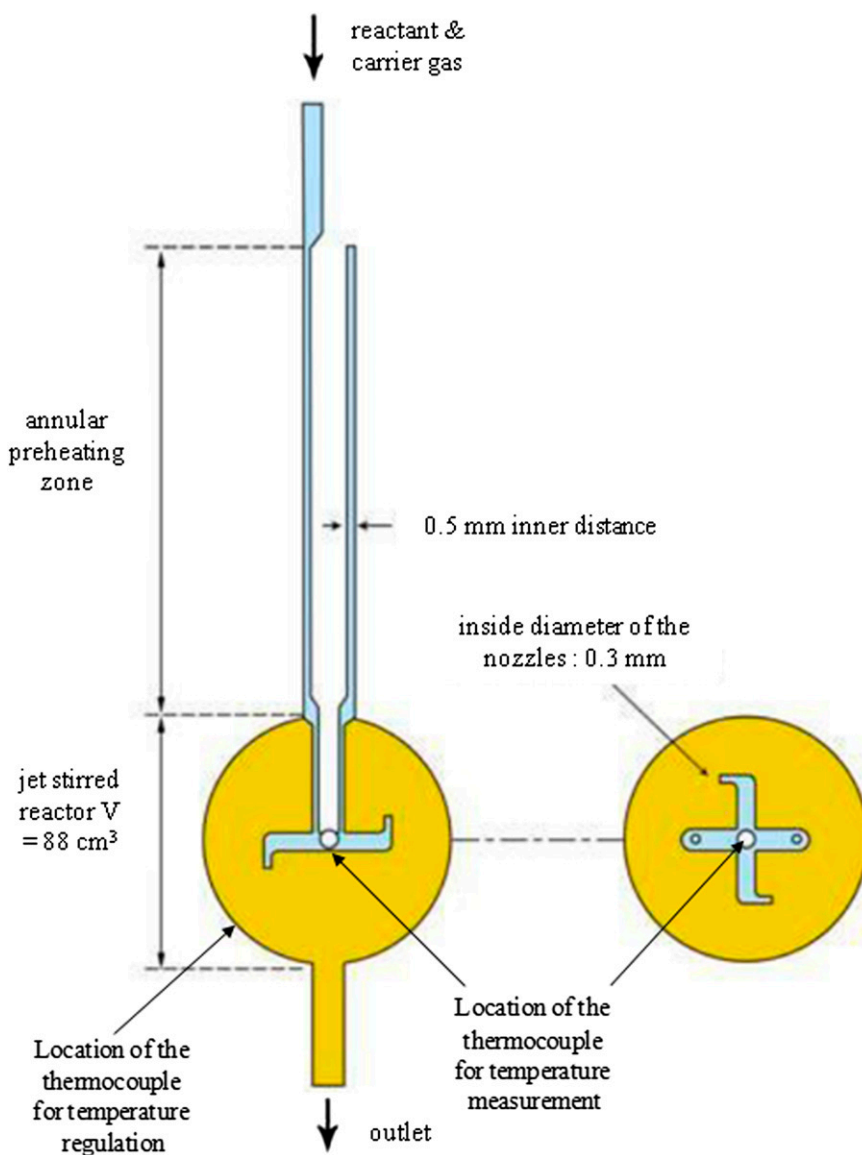


Fig. S1. Scheme of the JSR without the sampling probe.

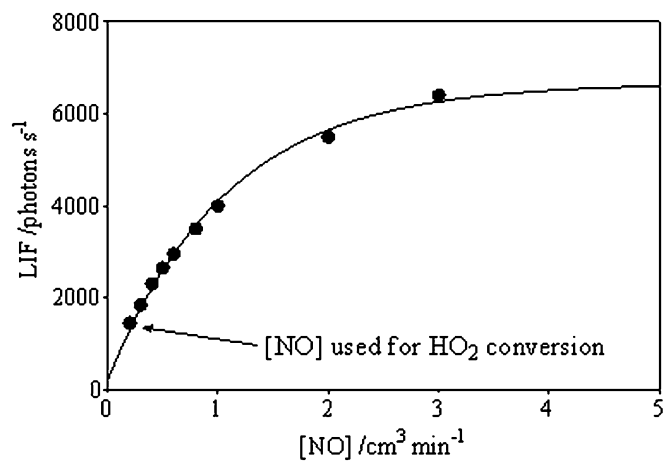


Fig. S2. Evolution of the fluorescence signal as a function of added NO concentration for an experiment at a JSR temperature of 643 K.

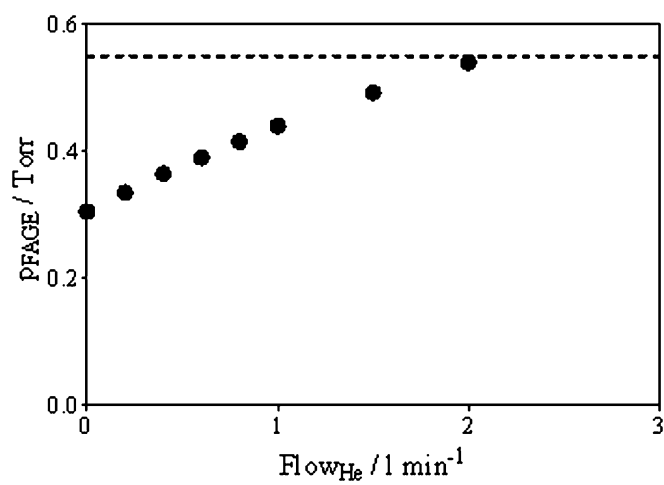


Fig. S3. Evolution of the pressure inside the FAGE cell with increasing He flow through the JSR.